Deformation and stress in PMMA during hard X-ray exposure for deep lithography

Nicolaie Moldovan*

Argonne National Laboratory, Advanced Photon Source, 9700 S Cass Av., Argonne, IL 60439

ABSTRACT

The availability of high-energy, high-flux, collimated synchrotron radiation has extended the application of deep X-ray lithography (DXRL) to thickness values of the PMMA resist of several millimeters. Some of the most severe limitations come from plastic deformation, stress, and cracks induced in PMMA during exposure and development. We have observed and characterized these phenomena quantitatively. Profilometry measurements revealed that the PMMA is subjected either to local shrinkage or to expansion, while compression and expansion evolve over time. Due to material loss and crosslinking, the material undergoes a shrinkage, while the radiation-induced decomposition generates gases expanding the polymer matrix. The overall dynamics of the material microrelief and stress during and after the exposure depend on the balance between compaction and outgassing. These depend in turn on the exposure conditions (spectrum, dose, dose rate, scanning, temperature), post-exposure storage conditions, PMMA material properties and thickness, and also on the size and geometry of the exposed patterns.

Keywords: LIGA, deep lithography, hard X-rays, stress, PMMA, radiation effects

1. INTRODUCTION

The way LIGA technology has established its place in micromachining is based on exposure with synchrotron radiation having critical photon energy in the 2 - 5 keV range. As resists, PMMA or other X-ray sensitive polymer layers were used because of their property to change solubility after exposure. Their thickness is in the range from microns to hundreds of microns.[1,2] For thicker resists, the exposure becomes difficult due to the absorption of the radiation in the material: the top of the resist is overexposed and damaged, while the bottom does not reach the threshold dose for being developed. To overcome this problem, one possibility is to use higher photon energy X-rays, which are not absorbed as well in the material. Since the material is less absorbent for this radiation, higher intensities or exposure times are also required to produce the same developing effect. The Advanced Photon Source of Argonne National Laboratory is able to generate high-flux, collimated synchrotron radiation with critical photon energies up to 20 keV and was used to expose PMMA layers of several millimeters thickness.[3-6] The extension of the technology towards ultra-deep X-ray lithography (UDXRL) encountered several difficulties, many of them already surpassed: the need for thicker absorbents in the masks,[4] problems with the developing of narrow holes, and adhesion problems.[6] One of the limiting factors in obtaining 1-5 millimeter-high structures is the development of cracks in the PMMA. Cracks can appear during or some time after the exposure; others appear after the developing. Most appear in the exposed zones after a partial developing and drying. The developers are alcohol-containing solutions, which are often used in the industry to test the induction of stress in objects fabricated of acrylics, because they produce severe cracks.[7] This is based on their stress-corrosion properties. Thus, the stress problem in the microstructures becomes even more critical during the developing process. Even in the case of complete developing, cracks can be observed sometimes on the sidewalls of microstructures. The stress induced by the hard X-ray radiation in the exposed areas of PMMA is manifest in the unexposed areas too, producing damage and limiting the performance of UDXRL.

Radiation is known to produce chain scission, crosslinking and material loss by outgassing in polymers.[8] PMMA was chosen as a proper X-ray resist due to the dominance of the chain scission effects. However, all the effects mentioned are present. They lead to the buildup of stress and to changes in the material properties after irradiation. To investigate the mechanical effects of hard X-ray synchrotron radiation in the PMMA, experiments were performed consisting of exposures with different X-ray doses and measurement of the evolution of the resist profile after the exposure. The visual aspect of the damage was

* Correspondence: Email: moldovan@aps.anl.gov; Telephone: 630 252 6263; Fax: 630 252 0161

DISCLAIMER

investigated using optical and electron microscopy. The analysis and discussion of the results led to a model able to explain and predict the evolution of stress in UDXRL microstructures.

2. EXPERIMENTAL

The exposure experiments were performed on the 2-BM beamline of the Advanced Photon Source of Argonne National Laboratory. The energy spectrum of the beam used is presented in Fig.1. A 1-mm-thick carbon filter was used to cut the low-energy part of the spectrum, and a 0.15° tilted chromium mirror was used to eliminate the high-energy part. To simulate the real conditions of exposure through a silicon substrate mask, an additional blank 300-μm-thick silicon wafer was inserted in front of the samples. As a mask, a 3-mm-thick steel plate was used, containing holes of diameters from 0.5 to 2 mm obtained by precision mechanical drilling. Different exposure doses were achieved by sequentially closing the slits during the scanning. This implies also that the lower dose exposures were finished earlier (up to some hours) than the higher dose exposures, but were done at comparable dose rate. The steel mask was placed 5 mm from the PMMA samples. The scanner chamber was connected to He at atmospheric pressure to enhance the heat exchange and to reduce the energy loss in the air. The exposures were done on 2-mm-thick PMMA plates (Goodfellow, Perspex CQ grade). The developing, when referred to, was carried out in a G-G system.[5]

During the exposures, the backside of the plates was in contact with the thermostated scanner plate, at 22°C. The evolution of the temperature during the exposure process was monitored in separate experiments, using thermocouples mounted in several points on the scanner, including the PMMA plates. The highest increase in temperature was observed on the mask itself (25-35°C), while the temperature difference between the inlet and the outlet of the He was about 3°C. The thermocouples on the PMMA plates (not mounted in the direct beam path) showed no more than 1-2°C increase during the exposure.

While the dose received by the samples varies from top to bottom, for, all the doses were calculated and expressed at the bottom of the 2-mm-thick PMMA. The profiles of the samples were measured using a Tencor 500 profilometer. To visually observe the samples, optical microscopy and SEM (R.J. Lee Instruments Ltd. PSEM) in the variable pressure, backscattering mode were used.

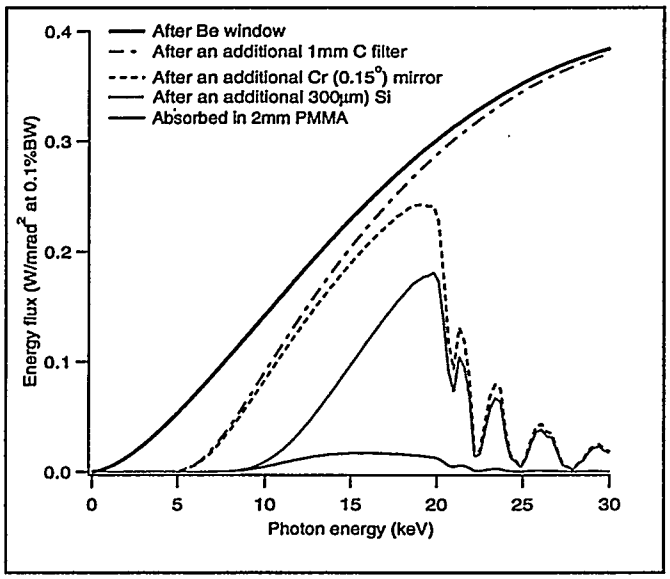

Fig.1. The energy spectrum of the beam at the exit through the Be window, after a 1mm C filter, reflection on the Cr mirror at 0.15°, and absorption in 300 μm Si. The energy absorbed in 2 mm PMMA is also shown.

3. PRIMARY OBSERVATIONS

A visual inspection of the samples shows a change in color of the exposed areas, which get a slightly amber tint. The intensity of this tint increases with dose, until bubbles of gas can be seen to form somewhere at 55-65 μm under the surface of the PMMA, at about 6000 J/cm^3 (Fig.2). The border of the exposed zones is visible already at very low doses (~1000 J/cm^3), as a small phase-shifting optical effect, denoting a local steep relief change. Later measurements concluded that this border really corresponds to the mask margins (Fig.3). The amber tint extends 50-70 μm outside this border and has a quite

abrupt margin rather than a gradual extinction. At about 7500 J/cm^3, the density of bubbles is so large that the PMMA looks like a foam. The dose at which bubble formation and foaming appear also depends on the size of the exposed area: smaller features form bubbles and foam at higher doses. Cracks appear right after or probably even during the exposure time only on large exposed areas. Between a few days to weeks later, cracks appear even in zones exposed to 4000 J/cm^3 also depending on the size of the respective zones. For the same feature size, the number of cracks and their size increases with dose. A very thick (5.6 mm) PMMA sample exposed with a dose of 7000 J/cm^3 at the surface showed cracks starting at about 0.35 mm under the surface and ending at a depth of about 3.5 mm. The amber colored material and especially that showing bubbles and foam are very brittle and can be easily damaged by a slight touch with a probe.

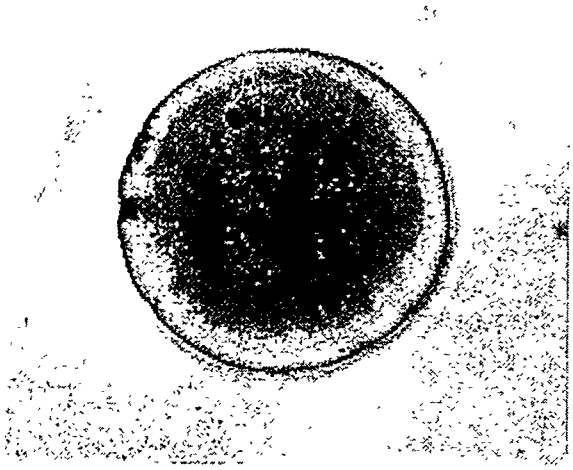

Fig. 2. Transmission optical micrograph of a 0.5-mm-diameter exposed zone, focused at 60 μm under the surface, showing the formation of bubbles. The exposure dose was 5570 J/cm^3.

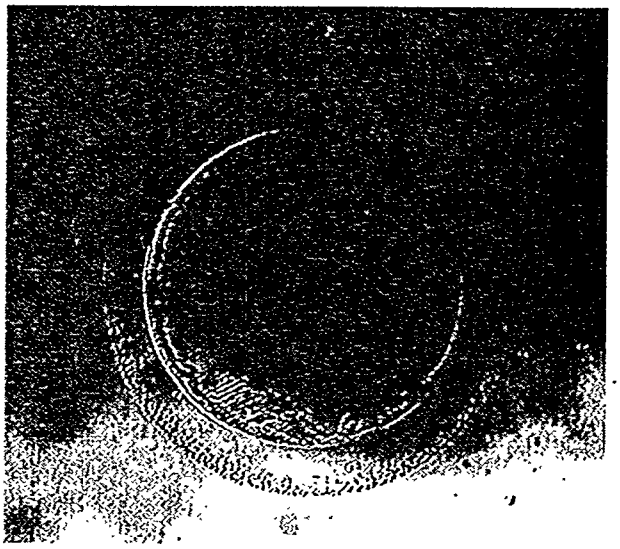

Fig. 3. Interference contrast optical micrograph of a circular exposed zone of diameter 0.5 mm showing the position of the border and the extent of the brown-yellow tint. Special image processing was used to enhance the contrast for a better view in black & white format.

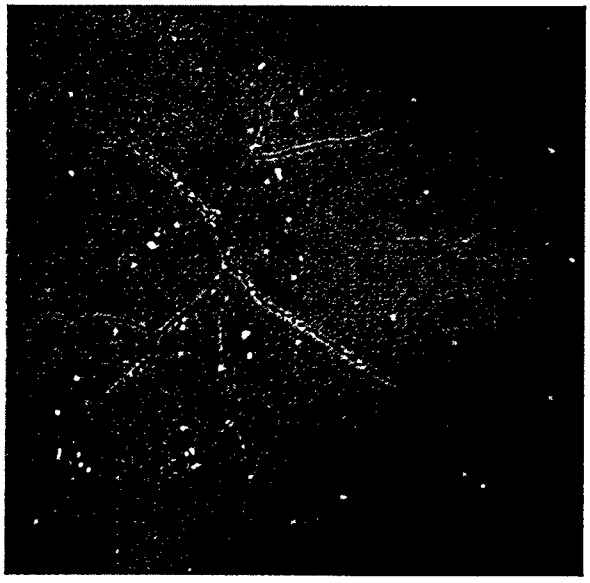

Fig. 4. SEM image of a 0.5-mm-diameter exposed area showing cracks at the surface taken 14 days after the exposure with a dose of 6809 J/cm^3.

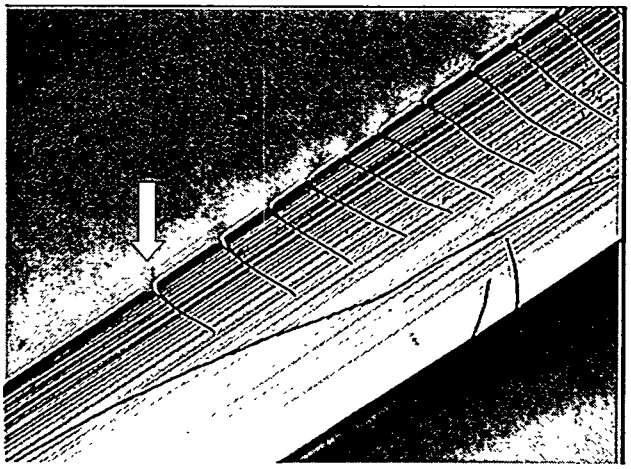

Fig. 5. A portion of the lower end of a UDXRL-fabricated columnar structure of a 100 μm square section of PMMA 1mm high, showing regulated cracks. The arrow points on the V-shaped end of a crack, the result of corner rounding during the dissolution process. Their regular aspect suggests they appeared due to a mechanical load upon the column, i.e., not before developing.

Several days after the exposure, cracks originating under the surface level extend towards the surface. They become visible at the top of the exposed areas (Fig.4). In case of developing, however, these areas are removed during the early steps of dissolution, suggesting that the top cracks are not critical. This is also sustained by the fact that the surface cracks are oriented perpendicular to the surface and hence are improbable to cross vertical structures. Much more critical are cracks that appear at the middle or lower part of the isolated structures, causing breakage in the developer or later on when the sample dries. These cracks appear during the developing process but are not visible until the sample is dried. Their appearance strongly suggests that they appear while in the developer. Fig. 5 presents an image of a part of a columnar structure of PMMA, 1 mm long and having a 100 μm square section. The structure shows typical cracks of similar length and orientation and having a very regular placement. The fact that all the cracks end at a well-defined depth in the structure indicates that they are not of the irregular type born prior to the developing. The small V-shaped outer ends of the cracks suggest they were already present in the developer, which acted to round their sharp edges. Hence, they must have appeared during the developing process and can be regarded as a stress-corrosion effect.

The significance of these observations will be discussed later in section 5.

4. EXPERIMENTAL PROFILOMETRY RESULTS

Several X-ray exposures were done with the beamline configuration previously described, exposing 2-mm-thick PMMA plates through a mask containing circular holes with diameters of 0.5, 1 and 2 mm. The profile of the surface was measured on the front and on the back of the plates, across the exposed zones. A first set of measurements was done between 1 and 8 hours after the exposure, while a second one was done two weeks later. The results are summarized in Figs. 6-9.

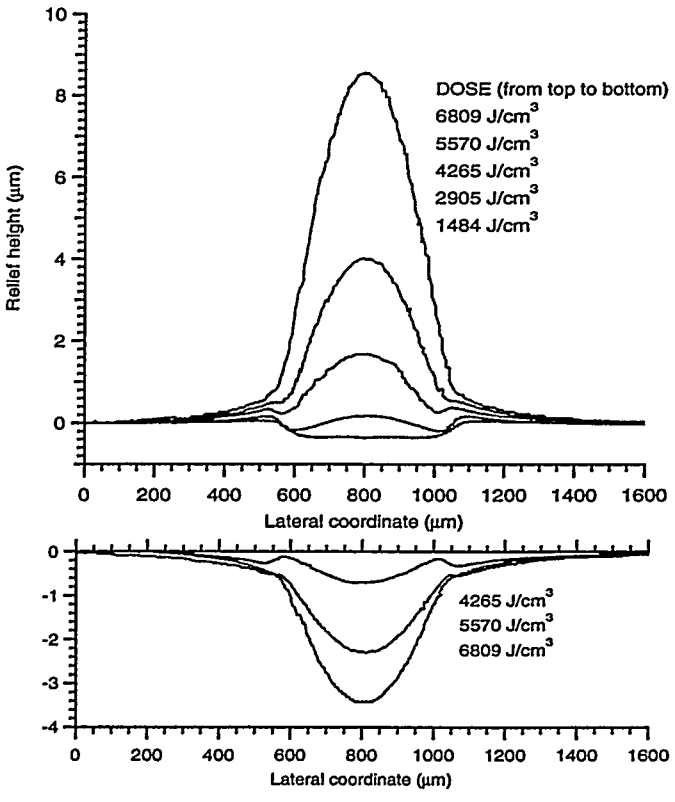

Fig. 6. Profiles of the 0.5-mm-diameter zone for different exposure doses, in the first hours after the exposure. Profiles on the front and on the back of the PMMA plate are represented. Dose values are expressed at the bottom of the 2-mm-thick plate.

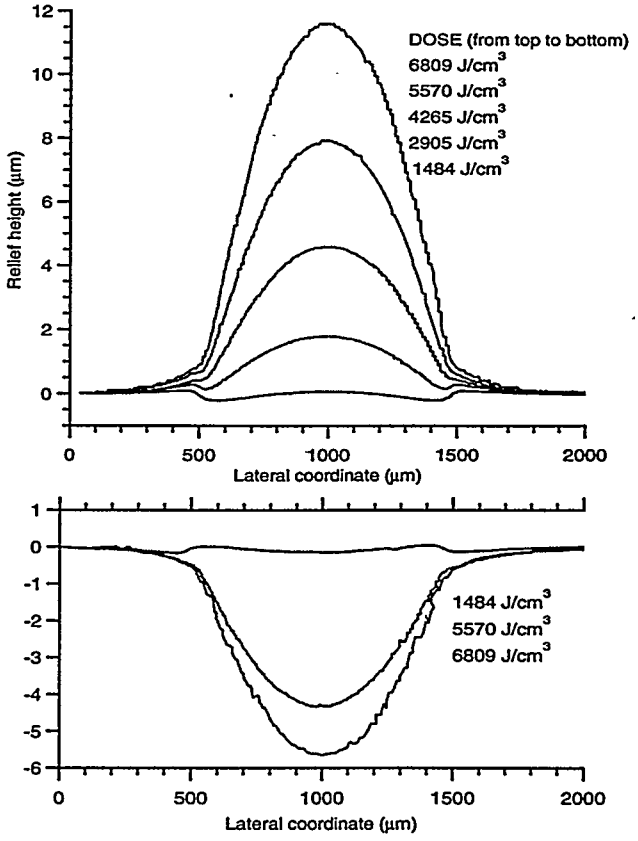

Fig. 7. X-ray-induced relief on the front and on the back of a 2-mm-thick PMMA plate. Mask: 1 mm circular hole. Doses expressed at 2 mm depth.

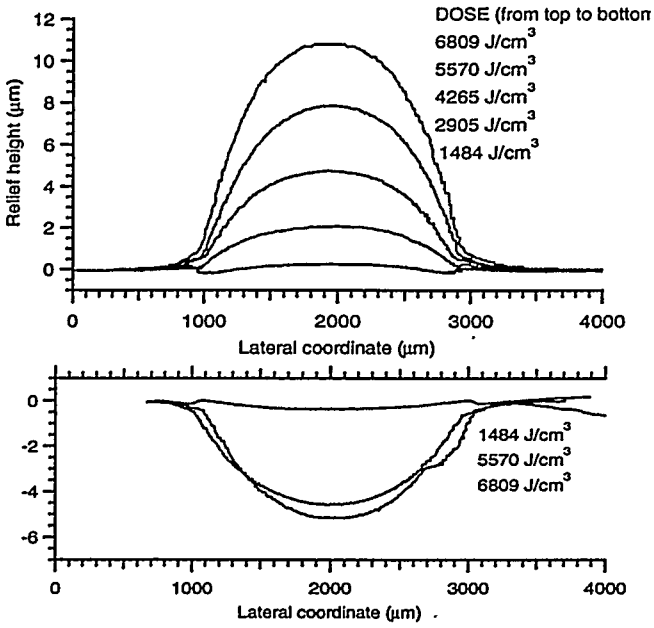

Fig. 8. X-ray-induced relief on the front and on the back of a 2-mm-thick PMMA plate. Mask: 2 mm circular hole.

Fig. 6 shows the profiles for several values of the dose for the 0.5-mm-diameter zone. Since increasing the dose corresponds to the evolution in time during the exposure, we can roughly get an idea about the dynamic of the surface. In the first steps of the exposure, there is a slight shrinkage of the surface of about 0.5 µm. After about 2500 J/cm^3, the middle of the zone starts to rise, ending at 6809 J/cm^3, at about 8.5 µm high. At exposures above 7500 J/cm^3, the material starts to foam and the surface rises irregularly and fast. Similar behavior can be noticed on the back of the plate, but there the evolution of the surface profile is delayed due to the fact that the actual encountered dose on the front of the PMMA plate is 29.7% higher, as one can calculate. If one takes this into account, the geometric effects on both sides are similar for the same local dose.

Figs. 7 and 8 show the case of the 1-mm- and 2-mm-diameter zones. Their behavior is totally similar to the case of the 0.5 mm structures, only the growth effect is greater. However, the total rise of the surface does not exceed 12 µm, showing a kind of growth saturation.

A common observation is that the material outside but close to the exposed area is also evolving, suggesting it is elastically strained by the growth of the center. However, the same thing does not happen in case of the shrinkage.

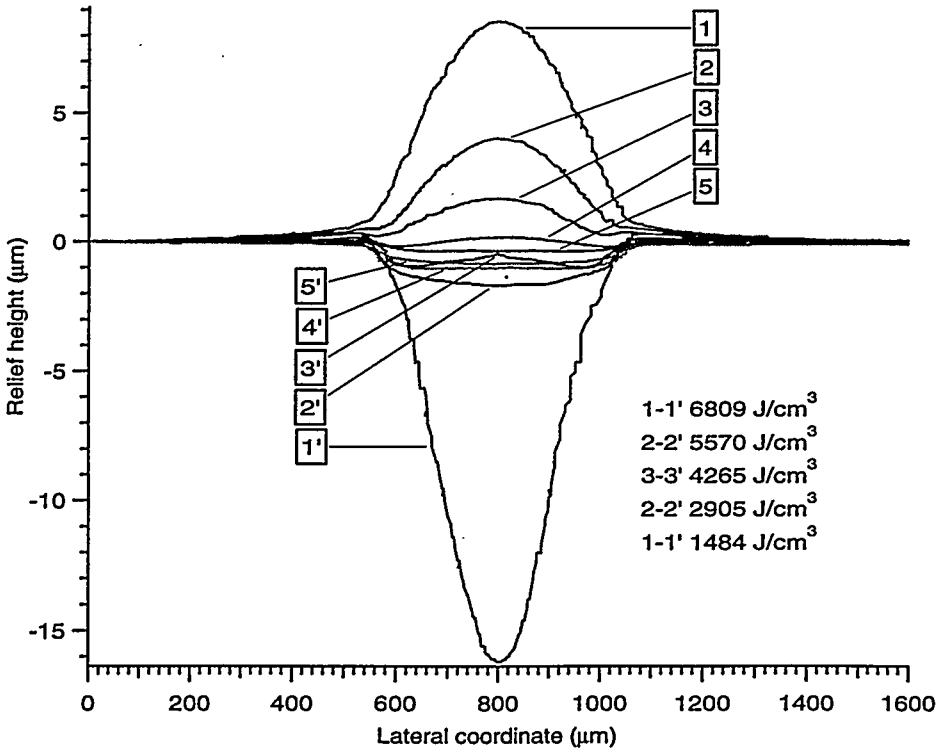

Fig. 9. The evolution of the profile of the 0.5 mm structures during two weeks.
1-5 are the profiles measured soon after the exposure, and
1'-5'are the profiles measured after two weeks. The profiles were measured on the front of the 2-mm-thick PMMA plate.

After two weeks, the profiles were measured again and showed totally different shapes. Fig. 9 shows the evolution of the upper profile of the 0.5 mm zone as a plot of pairs of profiles with different exposures. The protrusion transforms into a depression. The greater the height at the beginning, the deeper the depression at the end. This can be best seen on the curves noted 1 and 1', for the highest dose in this experiment, 6809 J/cm^3. The final depth is even more pronounced than the initial height. If one considers only the long-term effect, most of the relief change occurs between 5570 and 6809 J/cm^3. In this interval of dose, the depression deepens no less than 14.5 μm. Similar effects can be noticed on the back of the plates and for all the structure sizes.

5. DISCUSSIONS

PMMA is a material having a high yield of chain scission under irradiation. The chemical yield of radiation is defined as the number of events (i.e., crosslinking, scissions, recombinations, gas molecule or radicals emissions) per energy absorbed and is measured in μmol/J. A scission yield determined for PMMA is G(S)=1.63 μmol/J in vacuum and 0.77 μmol/J in air.[8] The crosslinking yield G(X) is practically not measurable. About the emission yields for different gasses, such as CO, CO_2, H_2, H_2O, CH_4, or heavier volatile components, the literature is poor. However, there is much qualitative evidence of the gaseous emission during irradiation, as evidenced by the bubbles in Fig. 2. Gravimetric measurements performed on large samples, uniformly exposed under the conditions mentioned in section 2, showed a weight loss of about 0.08-0.1 μg/J. This can give us an estimate of the amount of volatiles generated. Table 1 gives the values of the efficiencies of gas generation. We consider the whole lost mass to transform into one only gas species. Since the gas generated is a mixture of the species considered, the average volume of gas is a weighted average of the values given.

The possible scission reaction in PMMA induced by electrons or radiation was described[9] to have hydrogen as a main product. Thus, considering the high yield for chain scission, hydrogen should be one of the main components of the resulting gas mixture. This means the volume of the gas produced is expected to exceed the initial volume of the irradiated substance. Hence, a high compression is expected to appear.

Table 1. Maximal values for the gaseous emissions, considering the whole loss of mass transforms into one only species, for a mass loss efficiency in the PMMA of 0.1 μg/J.

Radiation efficiency for gas generation	Maximal value of efficiency (μmol/J)	Maximal volume in normal conditions of gas generated in 1 mm^3 of PMMA for a dose of 7000 J/cm^3 (mm^3)
$G(H_2)$	0.050000	2.84
$G(O_2)$	0.003125	0.49
G(CO)	0.003571	0.56
$G(CO_2)$	0.002273	0.36
$G(H_2O)$	0.005556	0.87
$G(CH_4)$	0.006250	0.98
$G(CH_3COOH)$	0.001667	0.26

Gas generation in the polymer matrix is significant not only because of material loss but also because of the accumulation of interstitial gasses in the polymer. The relatively uniform material loss in the polymer bulk due to formation of gasses and to diffusion, leaves space for the remaining polymer molecules to adapt their orientation for a better fit in the matrix. This is also enhanced by the fact that scission reduces the size of the remaining chains. The gaseous mixture undergoes a differential diffusion process. Some of the gasses reach the polymer surface and leave the matrix. The out-diffusion of the gasses is enhanced if the temperature is higher or the surface is closer. The portion of the remaining polymer undergoes shrinkage for which only the local material loss is responsible. This shrinkage appears as a depression on the surface and is a sign of the buildup of a tensile stress.

In the middle of the exposed polymer, the accumulation of interstitial gasses is dominant, leading to compressive stress. This stress is responsible for the volume expansion of the polymer-gas mixture and for the rise of the surface. Gasses also diffuse laterally, into the unexposed zone, producing compression. This explains why the surface also rises outside the exposed area. However, due to the fact that the surface material cannot be in a vertical compression (being free, the vertical component of

the stress tensor σ_{zz} has to vanish on the surface), the equilibrium in the material can be kept only if the surrounding unexposed polymer is in tensile stress. Because of the symmetry of the stress tensor, the situation will repeat in the horizontal plane for the radial and sagittal components of the stress tensor (σ_{rr} and $\sigma_{\phi\phi}$). The situation resembles a ball: when the air inside is in compression, the rubber is in tension. The difference is that, in the PMMA case, there is no homogeneity difference between the material that is in compression and the material that is in tensile stress. This situation is valid while the exposed zone is inflated by the gaseous irradiation products. However, in case the whole gaseous mixture leaves the polymer, its matrix obviously will remain in tensile stress. However, now the situation will be different: the outer part will be compressed, while the inner part will be in tensile stress.

These hypothetical scenarios apply only to the material at the very beginning and at the end of the process. In reality, the situation is always a mixture of the two, giving rise to a very complex evolution of stress and strain in the material. The real evolution can be understood only with the help of computer simulations, but this is a task for future research. The model described above is only to show that the stress in the exposed PMMA and its neighborhood have a complicated distribution and an even more complicated evolution, being related to the equilibrium between the matrix shrinkage and outgassing.

A rapidly achieved high-exposure dose will lead to accumulation of gases in the polymer matrix, exceeding the equilibrium saturation concentration. Thus, if the temperature of the material and the diffusion are kept low, an oversaturation, unstable quasi-equilibrium state can be reached. With time, bubbles of gas nucleate in the bulk, but their growth is diffusion limited and thus slow. Bubbles cannot appear very close to the surface, since there is always an opportunity for the dissolved gas from the surface to leave the material. This explains why bubbles were observed only at some depth in the polymer. Higher temperatures should lead to enhanced diffusion making the bubbles coalesce, and leading to fewer but bigger bubbles. This was observed for high-exposure doses, suggesting the temperature in those zones was higher. However, the *in situ* temperature measurements performed during exposures do not sustain this hypothesis. Alternative hypotheses are that the radiation directly enhances the diffusion process and highly exposed zones already have a looser matrix with a higher diffusion coefficient.

An estimation of the stress values appearing in X-ray-exposed PMMA can be made by observing the cracks and from profile measurements. By measuring the crack width and dividing it with the diameter of the exposed zone, one can obtain an idea about the strain value prior to breaking. SEM images of the type shown in Fig.4 can help in such cases. The estimates performed this way gave values of strain in the range 0.79 - 1.29 %. This is somewhat lower than the elongation at break reported for cast PMMA,[7] which is about 5.5%. However, the value is consistent with the fact that the exposed PMMA becomes more brittle. Considering a Young's modulus of elasticity for PMMA[7] of E = 3.3 GPa, the stress corresponding to the mentioned strain is in the range 26.2 - 41.9 MPa. These are values of stress and strain that would exist in the material, if undamaged; however, since cracks are already present, we may believe they appeared before this elongation was reached, i.e., our estimations are an upper limit for the tensile strength in the exposed PMMA.

The analysis of the surface profile can provide an evaluation of the compressive stress built into the PMMA by accumulation of gas, prior to the diffusion-based relaxation. A rigorous theory for determining the strain from the surface profile is under development. Here we will resume to some estimation but in good agreement with the overall observations. Considering roughly the neutral file passing through the middle of the PMMA plate, the relative overgrowth measured on the surface can give us an estimate of the gas-accumulation-induced strain. This is not an accurate measure of the strain, since the various components of the stress tensor are not independent. However, a first improvement can be achieved by considering the elongation not measured from the initial level of the PMMA plate but from the level it achieves after the outgassing. In the same way, the distance from the vertex of the relaxed (aged two weeks) profile to the initial surface level can be considered a measure of the compaction-induced absolute shrinkage. Multiplying the so-calculated strains by Young's modulus, one obtains the corresponding values of the stress. Fig.10 presents the plot of the calculated stress values as a function of dose at 2 mm, as a reference. The real dose at the level of the measured profiles is actually 29.7% higher.

As one can see, the compressive component ($\sigma<0$) induced by the gas accumulation has a threshold-type behavior, increasing substantially after 5500 J/cm^3. This is compatible with the model for oversaturation and nucleation of bubbles. The experimental points calculated from the total shrinkage, however, have a similar behavior. This is in contradiction with the fact that the compaction through material loss should be a linear effect of dose. Possible explanations are that the outgassing of some high-molecular-weight components was not complete at the time of measurement, or that Young's modulus of the exposed material increases with dose, leading to a nonlinear behavior. For this reason, as a more plausible dependence of the compaction effect on dose, we forced a line using the last point as a reference. In this case, the total stress in the material, summing the two effects, has a qualitative behavior that agrees with the observations made on cracks. Indeed, the peak of the

tensile stress reaches the tensile strength at about 30 MPa and a dose of 4-5 kJ/cm^3. The relaxation of the compressive stress through diffusion increases the tensile stress and the tensile strength can be reached even at 3 kJ/cm^3. This, obviously, gives more confidence in choosing the line for the compaction-induced stress the way it was done.

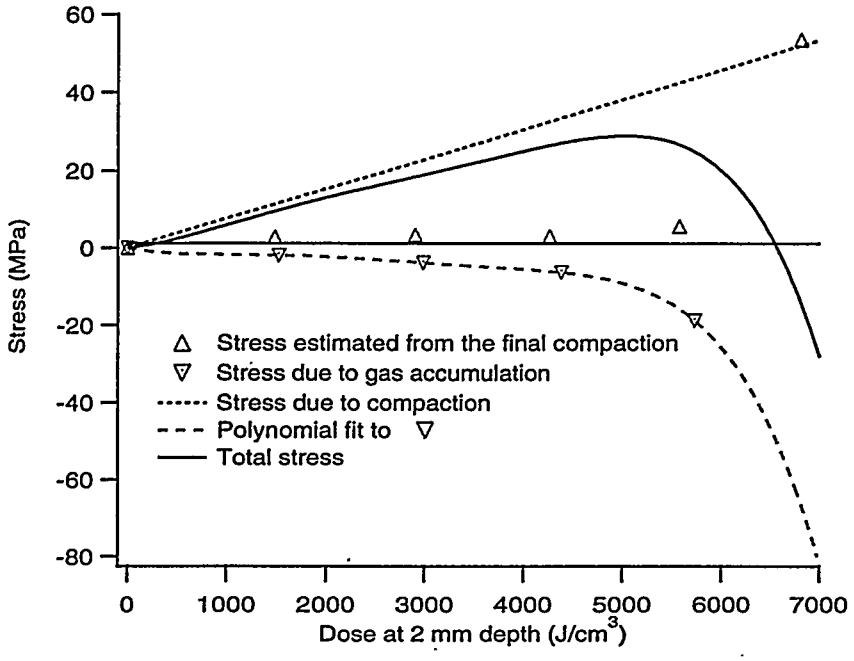

Fig. 10. Stress values estimated from profile measurements in the hard X-ray exposed zones.

A last comment should be made on the appearance of cracks of the type shown in Fig.5. A possible explanation is that the evolution of stress during the developing process continues. Due to the corrosion of material, stress has to be redistributed. Due to changing the boundaries for the diffusion process, the gas still present in the exposed zones can leave the material more easily. This can lead to a transient accumulation of tensile stress in some microstructures, exceeding locally the tensile strength of the material. The regular shape and placement of the cracks in the structure from Fig.5 shows the conditions of cracking repeat themselves periodically during the removal of the surrounding exposed material. This suggests once again that the UDXRL microstructures have to be stress-engineered taking into account various factors. The design of the masks can be probably optimized in many cases by adding dummy structures or choosing new positions for the structures.

6. CONCLUSIONS

Hard X-ray exposure of PMMA for UDXRL is strongly accompanied by development of stress in the material. Stress causes failure of structures through cracks. The investigation of cracks can yield information about the origin and evolution of stress. A systematic profilometric study performed by measuring the irradiation-induced relief in PMMA showed a local shrinkage of the polymer matrix superposed with a swelling. A few days after the exposure, the swelling retracts, resulting in an even higher shrinkage. The shrinkage was associated with material loss and scission of the polymer chain, while the swelling is a result of gas accumulation in the polymer. The size reduction of the swelling is explained by the outdiffusion of the gasses. The dynamics of the surface can give quantitative information about the complex evolution of stress and strain in the material. The evolution of stress continues during the developing process, leading to the appearance of specific corrosion-enhanced cracks. The stress engineering for UDXRL microfabrication will need special attention in the future.

7. ACKNOWLEDGMENTS

The author gratefully acknowledges Francesco DeCarlo for the valuable help with the X-ray exposures at APS/2 BM and Derrick C. Mancini for the stimulating discussions and remarks and for technical support of the experimental part. This work was supported by the U.S. Department of Energy, BES Office of Science, under contract no. W-31-109-ENG-38.

8. REFERENCES

1. B.Maid, W.Ehrfeld, J. Hormes, J.Mohr, D.Munchmayer, KfK 4579 report, 1988
2. T.R.Christenson, H.Guckel, Deep x-ray lithography for micromechanics", Proc. of SPIE Micromachining and Microfabrication Process Technology, Vol. 2639, (1995), pp. 134-145.
3. B. Lai, D.C. Mancini, W. Yun and E. Gluskin, "Beamline and exposure station for deep x-ray lithography at the Advanced Photon Source," SPIE Proc. 2880 (1996) p. 171
4. Philip Coane, Robert Giasolli, Francesco De Carlo, Derrick C. Mancini, Yohannes Desta, and Jost Göttert, "Graphite-based x-ray masks for deep and ultradeep x-ray lithography," J. Vac. Sci. Technol. B, (1998), pp 3618-3624
5. Francesco De Carlo, Derrick C. Mancini, Barry Lai, Joshua J. Song "Characterization of exposure and processing of thick PMMA for deep x-ray lithography using hard x-rays," Microsystem Technologies 4 (1998) pp. 86-88.
6. Francesco De Carlo, Joshua J. Song, Derrick C. Mancini, "Enhanced adhesion buffer layer for deep x-ray lithography using hard x-rays," J. Vac. Sci. Technol. B 16(6), (1998), pp. 3539-3542
7. H.Domininghaus, *Plastics for Engineers. Materials, Properties, Applications.*, Hanser Publishers, 1993, chapter 9, p. 278.
8. J.E.Mark, *Physical Properties of Polymers Handbook*, AIP Press, 1996, chapter 41.
9. O.Schmalz, M.Hess, R. Kosfeld, "Structural changes in poly(metyl methacrylate) during deep-etch X-ray synchrotron radiation lithography, Part II: Radiation effects on PMMA," Angewandte Makromolekulare Chemie, Vol. 239 (1996), p. 79